Investigation of Quasi-detonation Propagation Using Simultaneous Soot Foil and Schlieren Photography

Mark Kellenberger and Gaby Ciccarelli
Queen's University, Kingston, Ontario, Canada

1 Introduction

Flame acceleration in an obstacle laden channel can lead to steady propagation modes such as a fast-flame or a quasi-detonation wave. High-speed schlieren photography has been used in the past to show that the sub-CJ detonation measured average velocity is associated with a propagation involving repeated detonation initiation and failure [1,2]. The soot foil technique is typically used to record the detonation wave cellular structure, that consists of a "fish-scale" pattern of lines corresponding to the trajectories of the detonation front triple-points [3]. The soot foil technique has recently been used by Obara et al. [4] to investigate the DDT process in an a narrow channel with fence-type obstacles and by Starr et al. [5] to determine the cellular structure of a near-limit detonation waves in a round tube equipped with a schelkin spiral.

By definition a fast-flame propagates on average just below the theoretical isobaric speed of sound of the combustion products and a quasi-detonation propagates at an average velocity between the products speed of sound and the CJ detonation velocity [6]. High-speed schlieren was used to measure the explosion front velocity in a 7.6 cm tall by 2.5 cm wide channel equipped with equally spaced fence-type obstacles mounted on the top and bottom of the channel wall [2]. The average steady-state centerline velocity for stoichiometric hydrogen-oxygen at an initial pressure in the range of 8-30 kPa was obtained. Based on the average centerline shock velocity, and the details of the shock/flame (and detonation) interaction with the obstacles, five propagation modes were identified. The main differentiators between modes was whether ignition occurred at the obstacle face following shock reflection, and whether a detonation was initiated at the centerline of the channel following collision of the transverse compression waves produced by the local explosions at the top and bottom obstacles. The resolution of the schlieren images were not sufficient to identify the nature of the "local explosion" initiated at the obstacle face and at the channel centerline. The objective of this paper is to use simultaneous soot foil and schlieren photography to elucidate the propagation mechanism of a quasi-detonation wave. To the best of our knowledge the only time simultaneous soot foil and schlieren photography has been used was by Oppenheim in an obstacle free channel to "catch the detonation wave in the act of writing on the wall" [3].

2 Experimental

Experiments were carried out in an apparatus consisting of a 3.66 m long modular combustion channel with a cross-section of 2.54 cm by 7.62 cm. Along the length of the channel were "fence type" obstacles equally spaced at one channel height with a blockage ratio of 0.5. A Photron SA5 camera was used to take high-speed schlieren video in two different orientations, perpendicular to each other, see Figure 1. A 700 nm cut-off filter was used to block any infrared radiation produced in the test section.

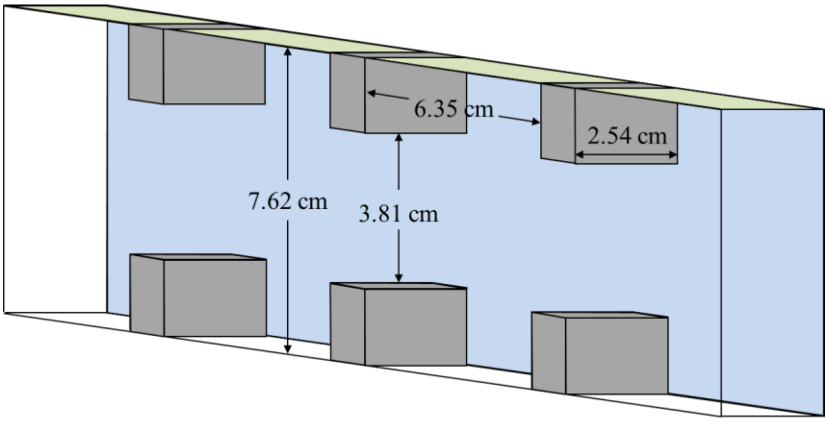

Figure 1. Obstacle geometry showing side video field-of-view in blue and top video field-of-view in green.

Videos were captured at up to 232,500 frames per second while simultaneously using the soot foil technique to obtain a physical record of the quasi-detonation propagation on the channel wall. This was accomplished by lightly sooting a thin sheet of glass with a kerosene lamp and placing it within the combustion channel, inside of the main 3.18 cm thick acrylic windows. A mixture of stoichiometric hydrogen-oxygen was used in all tests at an initial pressure of 9–30 kPa. The gaseous mixture was ignited from one end of the channel using an automotive capacitive discharge system.

3 Results and Discussion

High-resolution glass soot foils obtained at four different initial pressures are provided in Figure 2 and the measured centerline wave velocity obtained from the simultaneous video is provided in Figure 3. The direction of propagation is from right to left. There is no evidence of detonation cellular structure on the foil in Figure 2a, obtained at 9 kPa (mode 1 in [2] d/λ=2.0) and the wave velocity is consistently below the speed of sound, therefore the mode of propagation is a fast-flame. At each obstacle pair there is a "<" marking at the center of the channel produced by a pair of triple points on the shock front.

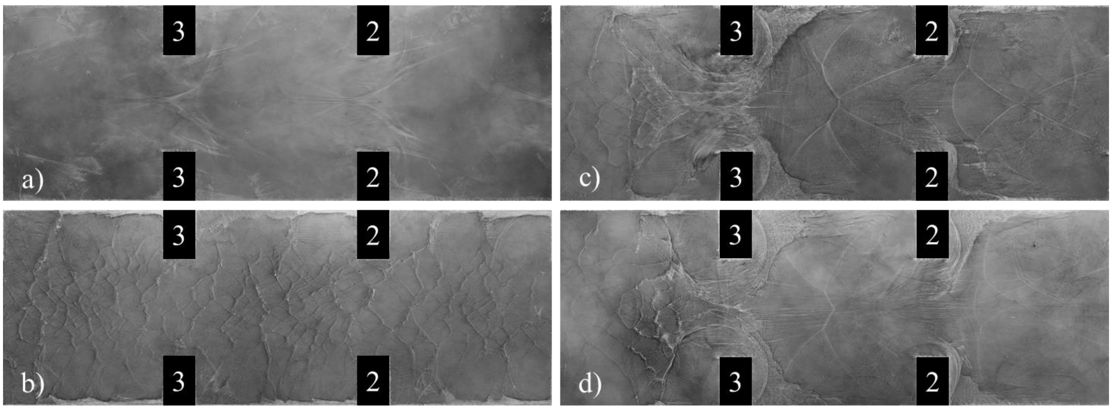

Figure 2. Soot foils obtained for stoichiometric hydrogen-oxygen: a) 9 kPa (test 1054), b) 30 kPa (test 1065), c) 15 kPa (test 1064), d) 12 kPa (test 1075).

The foil shown in Figure 2b, obtained at 30 kPa (mode 5 in [2] d/λ=11.9), shows a roughly uniform cellular structure. The centerline wave velocity oscillates about the CJ detonation velocity. There are very few cell directly behind each obstacle where detonation diffraction occurs, and slightly smaller cells after each obstacle at the channel centerline where reflected shocks from the obstacle pairs collide increasing the local pressure. For the 12 kPa (mode 3 or 4 in [2], d/λ=3.1) and 15 kPa (mode 3 or 4 in [2], d/λ=5.0), in Figures 2c and 2d, there are very fine cells located before obstacles 2 and 3 and cells form after obstacle 3 at the channel centerline, characteristic of detonation initiation. This indicates that a detonation wave is initiated at obstacle 3 following shock reflection. The detonation waves fail as they diffract around the obstacle corners, producing two shock waves that collide at the centerline initiating a detonation wave. The centerline velocity in Figure 3 shows a small increase in velocity after obstacle 2 and a large increase after obstacle 3 corresponding to detonation initiation.

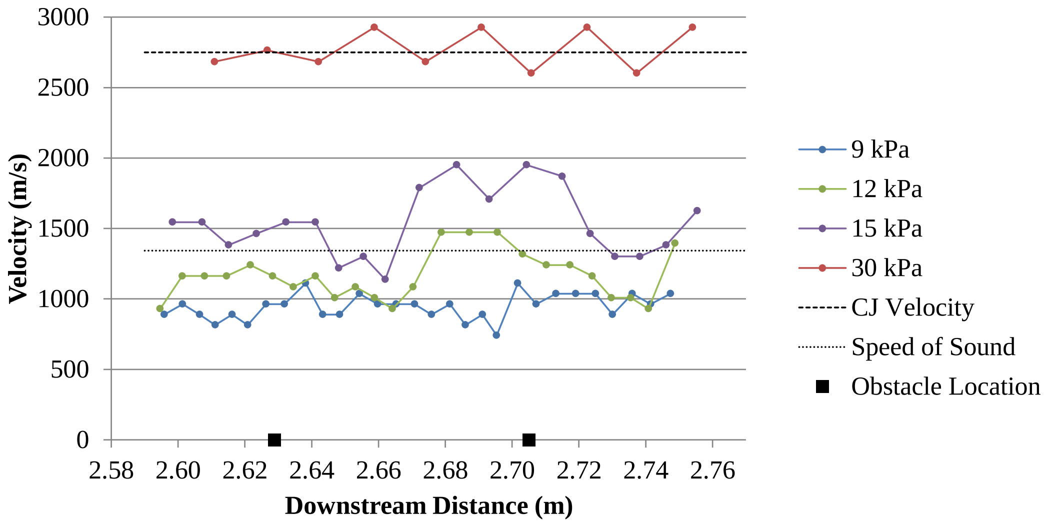

Figure 3. Centerline wave velocity obtained from simultaneous videos for tests in Figure 2 showing obstacles 2 and 3.

Figure 4 shows the soot foil and simultaneous schlieren video obtained from a test done at 15 kPa. The field-of-view for the video is shown as a dotted box overlaid on the soot foil, see Figure 4a. The right half of the field-of-view is not coated with soot. Shown in the field-of-view box are the three lines (denoted A, B and C) that are mirror images of dominant soot tracks recorded above the centerline.

The soot foil lines A, B and C are overlaid on select video frames in Figure 4c, and their significance will be discussed below. In the first image of Figure 4c, a shock wave (S) is located just before obstacle 2, immediately followed by the flame (F). The incident shock reflects off the bottom channel wall producing a small Mach stem and reflected wave (R in frame 2). Also in frame 2, the incident shock S reflects off the top-corner of obstacle 2 producing a reflected shock wave (R2). In frame 3 the Mach stem reaches the obstacle and R2 has propagated across the obstacle face reaching the corner. The convergence of R2 and the Mach stem produces a hot spot at the obstacle bottom-corner between frames 2 and 3 and a detonation wave (D) is initiated that travels radially out of the corner and a retonation wave (RW) travels back into the products in frame 5. The detonation wave fails as it diffracts around the top-corner of the obstacle resulting in a shock flame complex in frame 6. The shock wave travels to the channel centerline (a line of symmetry) where it interacts with the matching shock approaching from above (not in the field of view). This reflection produces a hot spot (frame 6) that transitions into a detonation wave (D2) in frame 7. The detonation wave sweeps across the front propagating in the pre-compressed gas between the decoupled shock wave and trailing flame. Once the detonation reaches the sooted part of the field-of-view in frame 8 it becomes luminous, where the spotty light emission corresponds to the triple-point locations. It will be shown that this light is associated with the thermal radiation from soot that is dislodged from the glass, heated by the high temperature detonation wave products. In frame 11 the section of the detonation wave near the centerline is clearly decoupled and thus the detonation wave has failed. In this same frame the decoupled shock wave interacts with obstacle 3. The resulting reflected shockwave interacts with the matching shock approaching from above the centerline, momentarily re-energizing the detonation wave in frame 12 but the decoupling is seen to continue in frames 13 and 14.

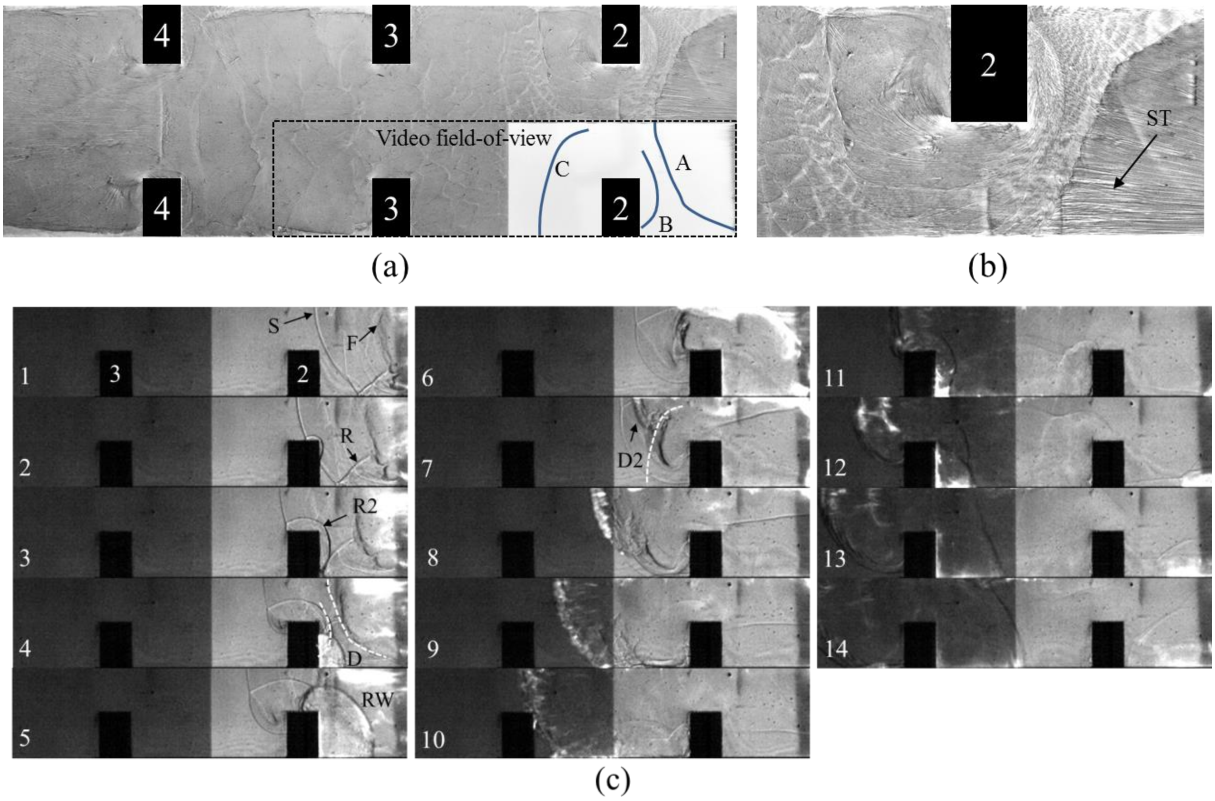

Figure 4. Test with stoichiometric hydrogen-oxygen at 15 kPa (test 1122). a) Soot foil, b) close-up of soot foil around obstacle 2, c) schlieren video (soot on left half of image) taken at 175,000 fps.

As discussed above following shock reflection, a detonation wave is initiated at the bottom-corner of obstacle 2 in frame 4. Very fine cells, associated with the overdriven detonation wave, originating at the hot spot location in the corner can be seen in Figure 4a and Figure 4b. The size of the cells increase with distance from the corner and is bounded on the right-hand-side by line A, (shown in Fig 4a) that corresponds to the flame location when it is traversed by the detonation wave in frame 4 of Figure 4c. Extra-fine cells are found inside the semi-circular region next to the obstacle, bounded by the position of the reflected shock R2 when it is traversed by the detonation wave (see frame 4 in Figure 4c). The divergence of the triple-point trajectories observed in Fig 4b indicates that the detonation wave fails as it diffracts around the upstream corner of obstacle 2. A detonation wave is initiated at the centerline (corresponding to the appearance of cells in Figures 4a and 4b). The fine cells associated with this detonation wave are bounded by the flame position (line C in frame 7 of Figure 4a). The overdriven detonation wave then decays in strength, with a corresponding increase in cell size approaching obstacle 3. The detonation eventually fails completely at obstacle 4 with the disappearance of the triple-point tracks. White streaks are observed on the soot foil leading up to the flame before obstacle 2 (ST on Figure 4b), as well as immediately downstream of obstacle 2. The streaks originate at large carbon particles deposited on the glass during the sooting process and are oriented in the flow direction. Interestingly the streaks do not appear in the path of a detonation wave, around obstacle 3.

Figure 5 shows the soot foil and simultaneous schlieren video obtained from a test done at 12 kPa. The phenomenon leading up to detonation initiation and propagation of the overdriven detonation across the obstacle face is similar to that discussed for the 15 kPa test in Figure 4. The difference is that the reflection of the decoupled shock wave at the centerline does not result in the formation of a detonation wave, as there are no cells on the foil at that location (Figure 5a and b). The initiation of the detonation at the bottom-corner of the obstacle is most likely governed by the chemical kinetics at the reflected shock condition. However, there are several factors that govern whether a detonation wave is initiated at the centerline, including mixture reactivity (initial pressure for these tests), height of the obstacle, and the amount of mixture that is detonated at the obstacle face following shock reflection. The amount of mixture that detonates is dictated by the separation distance between the shock and the trailing flame at the time of reflection (e.g., separation distance in frame 1 of Figure 4c is larger). Experiments where the separation distance can be controlled independently from the mixture reactivity and obstacle height need to be performed in order to investigate the critical initiation condition.

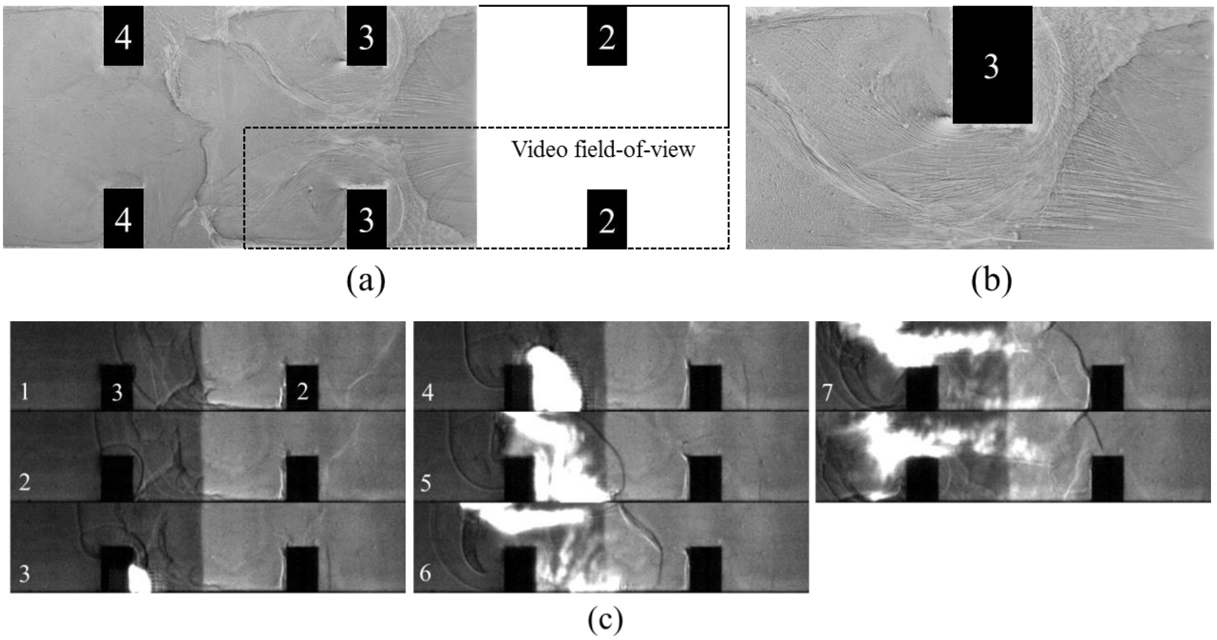

Figure 5. Test with stoichiometric hydrogen-oxygen at 12kPa (test 1080). a) Soot foil, b) close-up of soot foil around obstacle 3, c) schlieren video (soot on left half of image) taken at 175,000 fps.

Tests were performed with the channel geometry rotated 90° to get a top view of the channel (see green in Figure 1) in order to determine the 3-dimensionality of the detonation initiation and the effect of the soot on visible light production. Figure 6 shows video frames and a soot foil from a top-view test done at 15 kPa. Prior to obstacle 2, the shock (S) and flame (F) remain separated and relatively planar across the channel width. Upon collision with obstacle 2, a detonation is initiated at the top and bottom corners, indicated by the by the fine cellular structure visible on the upstream face on obstacle 2 in Figure 6a. From the side-view tests shown in Figure 4, this produces a transverse shock wave pair that collides at the channel centreline between obstacle pair 2, initiating a local explosion that transitions into a detonation wave, is characterized by the cellular structure seen starting at the centerline just downstream of obstacle 2 in Figure 6a. The video frames in Figure 6b indicate that this detonation is formed along a line, rather than at a point due to the uniformity of the resulting detonation in fame 11 but this is not universal. The detonation (D) propagates downstream and begins to fail after passing obstacle 3, characterized by the enlarged cellular structure on the left side of Figure 6a. Initially the detonation wave is overdriven and the cells cannot be seen in Figure 6b frame 11, but several triple-points can be seen across the channel in frame 15 after front weakening.

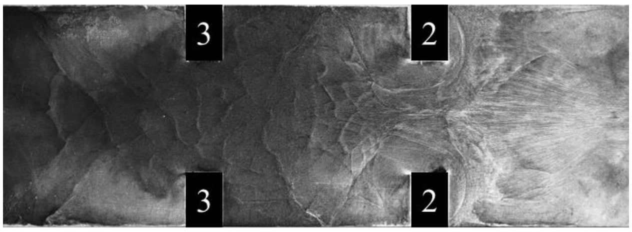

(a)

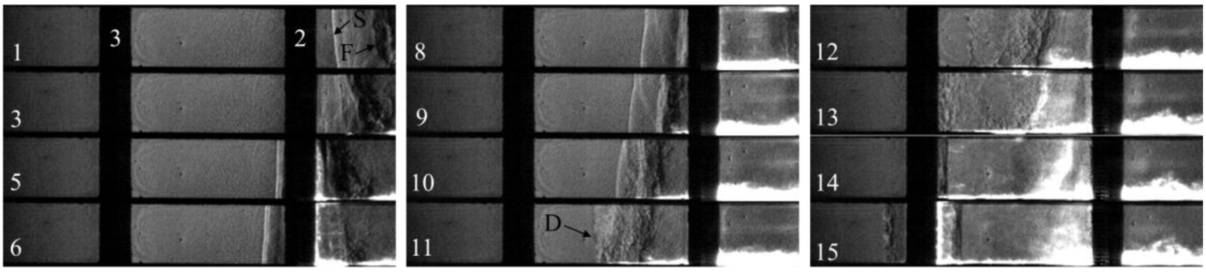

(b)

Figure 6. Test with stoichiometric hydrogen-oxygen at 15 kPa (test 1095). a) Soot foil, b) schlieren video taken at 232,500 fps with soot foil on the bottom channel wall.

The light produced along the bottom channel wall in Figure 6b is interesting as this is the location of the soot foil. The top wall (clean channel wall) does not emit the same intense light produced on the bottom (soot foil). Since only light rays that are parallel to the channel side make it into the camera (because of the schlieren set up), indicates that the light is emitted by the soot that is lofted from the foil and is heated by the combustion products.

4 Conclusions

Simultaneous high-speed schlieren and soot foils were successfully obtained of fast-flames and quasi-detonations propagating in a 7.6 cm tall channel with 50% blockage obstacles. The high resolution glass soot foils clearly show the fine cellular structure associated with overdriven detonation emerging from hot spots that form following shock collision at the obstacle face and the channel centerline. Simultaneous high-speed schlieren show the evolution of the shock/flame complex leading up to detonation initiation. Intense light is generated by the passage of the flame across a soot-covered surface. The heated soot particles radiate light in the visible spectrum.

References

[1] Teodorczyk A, Lee JH, Knystautas R. Propagation mechanism of quasi-detonations. Proc. Combust. Inst. (1988) 22:1723–1731.
[2] Kellenberger M, Ciccarelli G. Propagation mechanisms of supersonic combustion waves, Proc. Combust. Inst. (2015) 35(2):2109-2116
[3] Oppenheim AK. Dynamic features of combustion, Phil. Trans. R. Soc. Lond. A (1985) 315:471
[4] T. Obara, T. Kobayashi, S. Ohyagi, Mechanism of deflagration-to-detonation transitions above repeated obstacles, Shock Waves (2012) 22:627–639
[5] Starr A., Lee JH, Ng H. Detonation limits in rough walled tubes. Proc. Combust. Inst. (2015) 35(2):1989-1996
[6] Ciccarelli G., Dorofeev S. (2008). Flame acceleration and transition to detonation in ducts, Prog. Energy Combust. Sc. 34:499–550.